Check for updates

Dalton Transactions

An international journal of inorganic chemistry

rsc.li/dalton

Volume 46
Number 10
14 March 2017
Pages 3073-3412

ISSN 0306-0012

COMMUNICATION
Douglas W. Stephan et al
N-heterocyclic carbene stabilized parent sulfenyl, selenenyl, and tellurenyl cations (XH+, X = S, Se, Te)

ROYAL SOCIETY OF CHEMISTRY

ROYAL SOCIETY OF CHEMISTRY

rsc.li/dalton

ARTICLE

Bio-waste chitosan-derived N-doped CNT supported Ni-nanoparticles for selective hydrogenation of nitroarenes

Jacky H. Advani,[a,b] Krishnan Ravi,[a,b] Dhanaji R. Naikwadi,[a,b] Hari C. Bajaj,[a,b] Manoj B. Gawande[c] and Ankush V. Biradar [a,b],*

A facile method for the synthesis of leach proof and earth-abundant non-noble Ni nanoparticles on N-doped carbon nanotubes is reported. The catalyst was synthesized by an impregnation-carbonization method wherein the preformed Ni-chitosan complex upon carbonization gave under 5% H_2/N_2 at 800 °C yield Ni-containing N-doped CNT's. Chitosan served as a single source of carbon and nitrogen, and the nanotube growth was facilitated by the in situ formed Ni nanoparticles. The nanocatalyst was thoroughly characterized by several techniques; elemental mapping by SEM and TEM analysis confirmed the uniform distribution of Ni nanoparticles on the surface of N-doped CNT's with an average size in the range of 10-15 nm. The catalyst efficiently reduced a variety of nitroarenes (>99%) into corresponding amines under moderate pressure (5 bar) and comparatively lower temperature (80 °C). Furthermore, the easy recovery of the catalyst using an external magnetic field along with high activity and easy recyclability makes the protocol eco-friendly.

Introduction

The utilization of low-cost wastes like lignocellulose, bagasse, chitosan, etc. for the synthesis of carbonaceous supports/materials are imperative raw, and benign materials for advanced catalytic transformations. Among these, chitosan which contains ~40% carbon and ~8% nitrogen,[1] offers a direct route as a single precursor for the formation of *N*-doped carbon support. Of late, researchers have started utilizing this waste biopolymer for the synthesis of *N*-doped carbon materials for application in various fields.[2] The amino groups present in the principle skeleton of chitosan facilitate the chelation of metal ions to produce uniformly distributed metal nanoparticles. Among the several supports employed till date, carbon nanotubes (CNT's) have attained significant attention owing to its mechanical, thermal stability, and chemical inertness.[3] These CNT's are generally synthesized by catalytic a laser vaporization method,[4] chemical vapor deposition (CVD),[5] flame synthesis,[6] or electric arc discharge method.[7] These easily oxidizable nanotubes are in nano-dimension, which again stabilizes the dispersion of the metal nanoparticles. To further enhance the application of these CNT's, they are doped with heteroatoms such as nitrogen, sulphur, etc. Among the

reported heteroatom-doped CNTs, *N*-doped CNT's have raised to become one of the most promising supports due to their high surface area, enhanced mechanical, electrical, chemical and functional properties.[8] The introduction of nitrogen induces defects and provides active sites on the surface of the carbonaceous supports.[8] It also offers additional electrons to induce a negative charge on the adjacent carbon atoms upsurging the *p*-binding ability and basicity, the local charge density of the nanotubes, reduced resistivity and electron transport properties of the CNT's.[9] The nanoparticles immobilized on these materials are usually found to be much more stable as compared to the non-doped carbonaceous materials. This may be attributed to the electronic and structural promoting effect of the doping.[10]

Hydrogenation of various nitroarenes results in the formation of industrially important aromatic amines in pharmaceuticals, agrochemicals, fine chemicals, dyes, polymers, etc.[11] This has been achieved using various procedures involving the use of metal catalysts and using various reductants.[11] The chemoselectivity towards an aminated product in the presence of other reducible functionalities is still a challenge in the chemical industry. Additionally, hydrogenation of nitroaromatics often gives intermediary compounds like hydrazines, hydroxylamines, azoarenes, and azoxyarenes.[12] Precious metals like Pt, Pd, Rh, Ir, Au, etc.[11b, 12a] are routinely used for the hydrogenation of various nitro substrates. However, the limited availability of these metals and high prices largely influence the cost of the final products. Thus, researchers have shifted their focus intensively on the use of low-cost earth-abundant metals like Fe, Co, Ni, etc. [12c-12f] to develop an efficient hydrogenation protocol. Among the various metals used, Ni is the most widely used

[a.] Inorganic Materials and Catalysis Division, CSIR-Central Salt and Marine Chemicals Research Institute (CSIR-CSMCRI), G. B. Marg, Bhavnagar-364002, Gujarat, India. Email: ankush@csmcri.res.in

[b.] Academy of Scientific and Innovative Research (AcSIR), Ghaziabad-201002, Uttar Pradesh, India.

metal-based catalyst with price as low as 1/5000 to that of gold. Regardless of the huge success of this metal in industry, these single-component catalysts are inefficient in meeting the activity, selectivity, and stability to be applicable in the fields relating to energy and environment. Owing to the low catalytic activity of Ni-based catalytic systems, the hydrogenation reactions are ~~were~~ conventionally performed at a higher temperature and H_2 pressure.[13] Since the exposed surface area plays a vital role in ~~the~~ catalysis, the use of nanoparticles, which is known to provide high surface area, has become a reasonable elite for direct hydrogenation reactions.[2d, 14] However, due to the high surface area, these nanoparticles reduce their surface energies via agglomeration, slowly diminishing the catalytic activity of the catalyst. Also, ~~the~~ catalysts with the metals like Ni and Co tend to deactivate by sintering or via leaching.[15] Therefore, it is imperative to tailor-make a catalyst that is stable, easy to handle and also retains its activity, which has been accomplished by immobilizing the nanoparticles onto interactive supports that not only help in stabilization but also improve the catalytic activity.

A few reports on the synthesis of Pd nanoparticles supported on various composite materials with chitosan-derived *N*-doped carbon as one of the component have been reported.[2a-2d] Wang *et al.* reported the hydrothermal synthesis of Pd nanoparticles on composite support comprising ~~of~~ TiO_2 and chitosan-derived *N*-doped carbon for the hydrogenation of vanillin using formic acid as a hydrogen source.[2a] The report discusses the formation of Pd in various chemical states dispersed across the composite support. The material successfully hydrogenated vanillin to 2-methoxy-4-methylphenol with ~~an~~ excellent activity, which was attributed to the synergy between the Pd/TiO_2 and Pd/N-C interactions in the material. The Pd nanoparticle stabilized on montmorillonite-*N*-doped carbon composite at different carbonization temperatures was studied for the Heck coupling reaction.[2b] Notably, the thermal stability of the composite increased with the carbonization temperature. A similar kind of material was synthesized by carbonizing cobalt salt with chitosan resulting in the formation of $Co-Co_3O_4$ and was utilized for the chemoselective hydrodehalogenation of alkyl and heteroaryl halides.[2c] Recently, we reported the synthesis of highly dispersed and stable palladium nanoparticles on *N*-doped carbon via pyrolysis of the chitosan-Pd complex for the hydrogenation of various functional groups.[2d] The in situ formation of Pd nanoparticles, by the reducing gases evolved during controlled pyrolysis of chitosan, involved stronger interaction with the *N*-doped carbon support, thus giving a stable and highly dispersed catalyst. Inspired by the excellent results, we followed a similar synthetic method to synthesize nickel nanoparticles on *N*-doped CNTs via pyrolysis of Ni impregnated chitosan for the hydrogenation of various nitroarenes at lower reaction temperature and H_2 pressure as compared to the conventional protocols using higher temperature and H_2 pressure. The use of molecular hydrogen as a reductant at relatively low pressure has an added advantage as it does not produce any byproducts making the process benign.

Experimental

Fabrication of Ni nanoparticles on N-doped CNT (Ni@NCNTs). The synthesis of the Ni@N-CNT nanocatalyst was achieved by ~~an~~ impregnation followed by a pyrolysis technique. In a 250 mL beaker, 0.652 mg of $Ni(NO_3)_2 \cdot 6H_2O$ was dissolved in 50 mL of methanol. Around 10 g of chitosan was added to this solution under stirring and heated at 50 °C until all the methanol evaporated and dried. The resulting nickel adsorbed chitosan flakes were directly carbonized in a tubular furnace by slowly raising the temperature at a heating rate of 5 °C min^{-1} up to 800 °C under a 5% H_2/N_2 flow (10 mL/min). The black carbonized material (Ni@N-CNT) was powdered and stored in a tightly stoppered bottle and used as a catalyst for the hydrogenation reactions.

General procedure for catalytic hydrogenation reactions. In a 50 mL Parr reactor, 0.2 mmol of nitroarene, 20 mL solvent, tetradecane as the internal standard and the catalyst were charged followed by flushing with nitrogen gas to ensure removal of air. The reactor was pressurized with molecular H_2 and the temperature was raised as required followed by stirring at 800 rpm. ~~The~~ A constant supply of hydrogen gas was maintained during the complete reaction. The reaction was terminated when there was no noticeable drop in pressure, and the reactor was brought to room temperature and depressurized. The catalyst was separated from the reaction mixture and stored for further use, and liquid samples were used for GC/GC-MS analysis.

Recyclability and leaching analysis of the catalyst. The recyclability of the catalyst was ensured using nitrobenzene hydrogenation using a Ni@N-CNT nanocatalyst under ~~the~~ standard reaction conditions, i.e. 2 mmol nitrobenzene, 5 bar H_2, 20 mL Methanol, 80 °C and 800 rpm as a model reaction. The catalyst was separated using an external magnetic field, washed and dried at 50 °C after the completion of ~~the~~ reaction. This catalyst was reused for the next catalytic cycle under identical conditions, while ~~the~~ Ni leaching was ensured via ICP-OES analysis of the reaction mixture.

Result and Discussions

Synthesis and characterization of the catalysts. The gram-scale synthesis of the Ni@N-CNT nanocatalyst was achieved ~~in~~ via impregnation-carbonization of nickel salt adsorbed chitosan (Scheme 1). Owing to the glucosamine and acetyl glucosamine units, chitosan can easily chelate and stabilize the metal ions.[1a, 1c, 16] These metal ions interact with the carbon surface acquired via pyrolysis of chitosan and form Ni_2C[17], which is finally reduced to Ni nanoparticles during the carbonization process in the presence of 5% H_2/N_2 forming of uniformly distributed active Ni nanoparticles on porous *N*-doped carbonaceous surface. To date, the synthesis

ARTICLE

carbon nanomaterials with 1D architecture from the raw biomass precursors remains an immense challenge. The carbonization of chitosan at higher temperatures results in the formation of a graphitized carbonaceous structure.
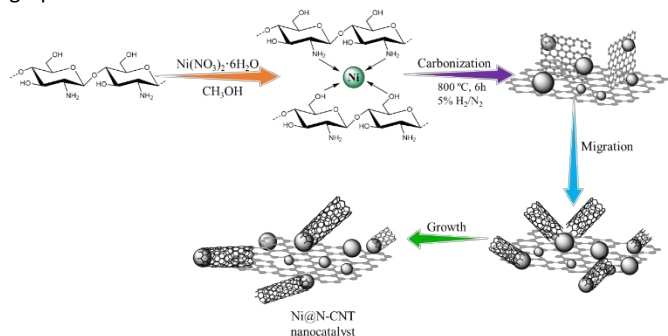
Scheme 1. Synthesis of Ni@N-CNT nanocatalyst by impregnation-carbonization method.

These graphitic carbon layers migrate towards the Ni nanoparticles, which act as the active metal center and start depositing on the surface of these nanoparticles resulting in the formation of nuclei. The process of carbon migration continues which results in the formation of hollow *N*-doped CNT's with anisotropic and distorted patterns. The nanoparticles thus formed are located at the opening end of these hollow CNT's. The retained nitrogen in the resulting support results in a higher dispersion of nanoparticles by stabilizing the nanoparticles and thus maintaining the catalytic activity of the material. It was found that the Ni nanoparticles formed *in situ* play a major role in the formation of microstructured carbon nanotubes with a high graphitization degree. Initially, the nickel salt was dissolved in methanol, followed by the addition of chitosan with continuous stirring. The chitosan starts to adsorb the nickel ions. Slowly, the temperature was raised along with continuous stirring until all the methanol evaporates, resulting in greenish-yellow flakes of the Ni-Chitosan complex. This material was then carbonized ensuing in the formation of black powdered material (abbreviated as Ni@N-CNT), stored in an airtight bottle and characterized by different physicochemical methods.

The morphology of the Ni@N-CNT nanocatalyst was obtained by FESEM images (Figure 1a-c). The FESEM image revealed discrete worm-like curly carbon nanotubes, which is amorphous nature with porous morphology. The growth of the nanotubes arising from the carbonaceous material can be easily viewed in Figure 1b. The nickel nanoparticles, formed during carbonization, located at the epitaxial end of the nanotubes promote the growth of these C-N nanotubes. The encapsulation of these nanoparticles at the top end of the nanotubes can be seen in Figure 1a-c. The nickel nanoparticles formed ~~are~~ were uniformly distributed with relatively less agglomeration (formation of larger nanoparticles). Furthermore, the elemental mapping of the catalyst showed a uniform distribution of C, N, O and Ni nanoparticles, which indicates the stabilization of the nanoparticles onto the carbonaceous support (Figure 1d-h). The energy dispersive X-ray (EDX) spectra of the Ni@N-CNT nanocatalyst (Figure 1i) confirmed the presence of C, N, O and Ni elements in the catalyst.
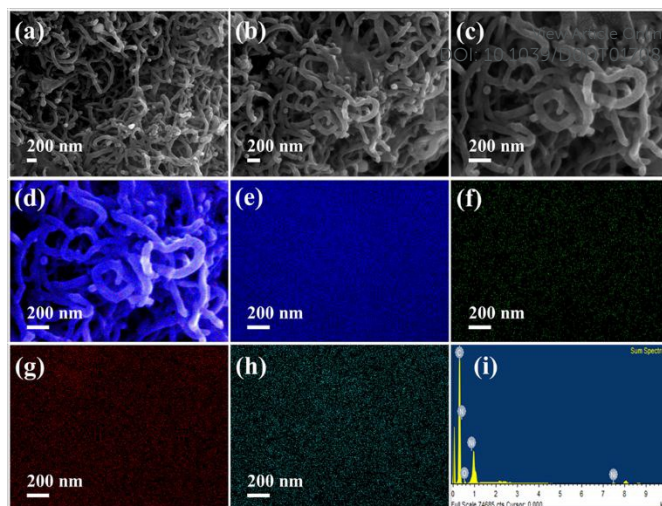
Figure 1. (a-c) FESEM image of Ni@N-CNT nanocatalyst at different magnification, element mapping of (d) Mix image for C, N, Ni and O, (e) Carbon, (f) Nitrogen (g) Nickel (h) oxygen and (i) EDX spectra of Ni@N-CNT nanocatalyst.

The topography of the synthesized Ni@N-CNT nanocatalyst was further characterized by TEM and HRTEM images (Figure 2). Figure 2a shows the carbon nanotube clusters formed along with the graphitic layer formation. The growth of the carbon nanotubes from the carbonaceous layer can be seen in Figure 2a-b and a completely grown CNT observed (Figure 2b). A broad particle distribution of nickel nanoparticles onto the *N*-doped carbon multiwalled nanotube (marked by arrows) with open end/mouth was ~~is~~ observed (Figure 2c). The average particle size of the Ni nanoparticles was found to be in the range of 10-15 nm. Figure 2d shows the formation of separate graphitic sheets responsible for the formation of the CNT's. Single multiwalled nanotube with an open-end/mouth with 4-6 nm thickness is observed in Figure 2e. These results confirm the formation of a graphitic carbonaceous material and CNT's grown from therein encapsulating the Ni nanoparticles. Notably, a Ni nanoparticle with the interplanar spacing of 0.20 nm is noticed which is in close agreement with the standard lattice fringes corresponding to the (111) plane of *fcc* structured Ni (Figure 2f). The elemental mapping of the catalyst is shown in Figure 2g-k. The uniform distribution of the C, N, O and Ni elements showed the effective doping of nitrogen in the resulting CNT's. The presence of the nickel single atoms on the CNT's yet again confirms the stabilization of ~~the~~ Ni owing to the *N*-doping in the CNT's. The amorphous nature of the material can be confirmed from the fused rings in the selected area diffraction pattern (Figure 2(l)) of the Ni@N-CNT nanocatalyst. The SAED pattern showed the presence of bright annular spots relating to the phase pure Ni metal which is consistent with the XRD analysis. The d-spacing of 0.5 nm relating to the high curvature carbon layers surrounding the nickel nanoparticles can also be observed in the SAED pattern.[2a]

ARTICLE   **Journal Name**
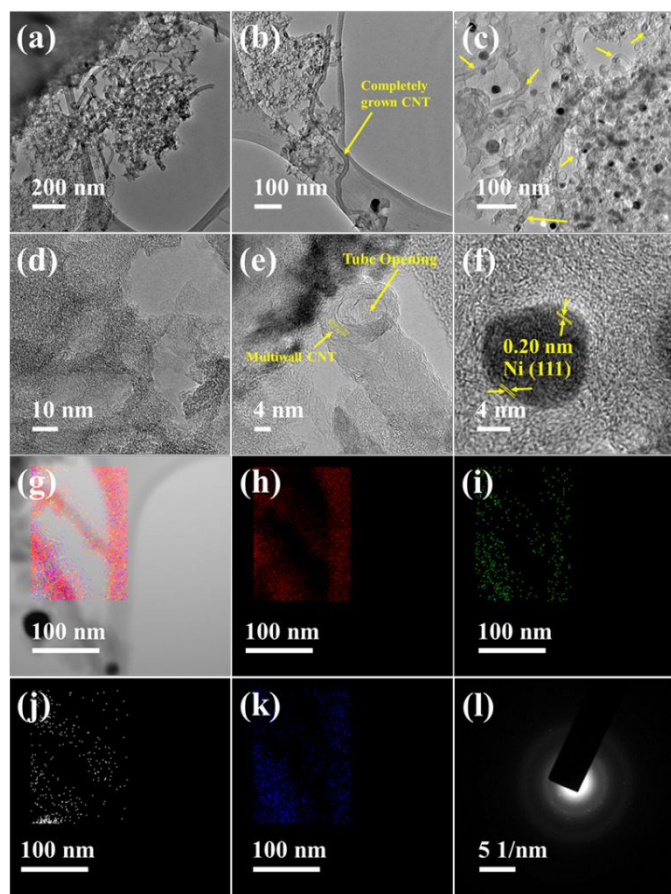
Figure 2. (a-c) TEM image of the Ni@N-CNT nanocatalyst. (d) HRTEM image of the graphitic carbonaceous sheet in the synthesized nanocatalyst (e) HRTEM image of the multiwalled nanotube with mouth opening. (f) HRTEM image single Ni nanoparticle. Elemental mapping of (g) mixture of C, N, O and Ni, (h) Carbon, (i) Nitrogen, (j) Nickel, (k) Oxygen, (l) SAED pattern of Ni@N-CNT nanocatalyst.

The carbonaceous nature of the materials was confirmed by Raman spectroscopy (Figure 3), where in-plane vibrations of the sp^2 carbon give rise to a band at ~1570 cm^{-1} known as the G band while the disordered carbon with the sp^3 electronic structure of graphitic carbon gives rise to a band at ~1340 cm^{-1} known as the D band (Figure 3a).[18]
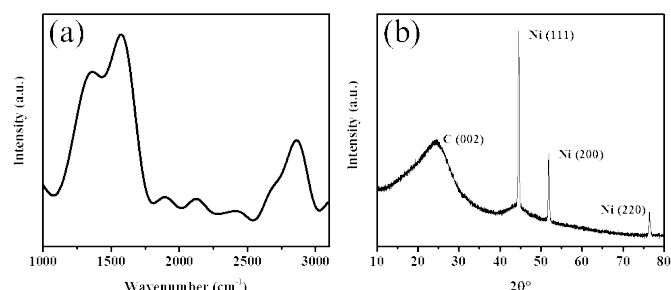

Figure 3. (a) Raman spectra of *N*-doped Carbon and Ni@N-CNT and (b) PXRD pattern of Ni@N-CNT.

The G band is ascribed to the tangential stretching of the C=C bond in a graphitic material relateding to the vibration originating from the sp^2 hybridized carbon atoms in the hexagonal 2-D lattice.[19] The presence of an overtone of the D band at 2850 cm^{-1} corresponding to the D+G band is the characteristic of the CNT.[20] The misalignment of the *p*-orbitals of the carbon atoms coupled together induces a strain due to the curvature, thus giving vibrations that are reflected as bands in the Raman spectrum. Such features are attributed to the defects and or vacancies that arise from the interaction/chemical bonding of the Ni nanoparticles and *N*-doped carbon during the carbonization process. Thus, we can confirm the formation of the graphitic nanotubes.

The PXRD patterns of the *N*-doped carbon and Ni@N-CNT display the peak at 2θ = 25° in both the support and Ni@N-CNT was observed, which can be attributed to (002) phase of the randomly oriented, aromatic, amorphous graphitic carbon (Figure 3b). The reflections at 2θ = 44.57°, 51.93°, 76.38° confirmed pure crystalline metallic nickel phases (111), (200) and (220) in the material (JCPDS no. 040850) with no NiO formation.[15,21] The crystallite size of the nickel nanoparticles using the Scherer's equation was calculated and found to be ~50 nm which is well under the nanoscale boundaries.

The high-resolution XPS spectra of the Ni@N-CNT nanocatalyst is shown in Figure 4. The characteristic signals of C, N, O and Ni elements were observed in the survey spectrum (Figure 4a) in the full range of 0-1100 eV. The deconvolution of the carbon spectrum showed three types of carbon peaks and characteristic of the graphitic carbon at 284.5 eV as a result of successful pyrolysis ensured graphitization (Figure 4b).
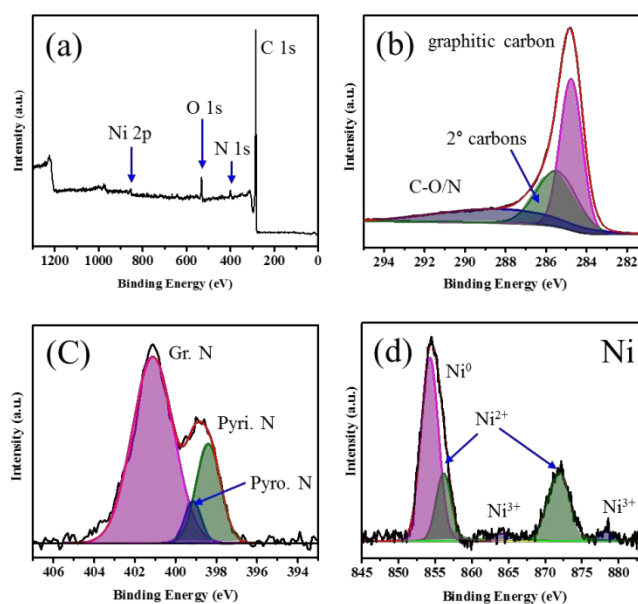
Figure 4. (a) Survey spectra of Ni@N-CNT nanocatalyst, High-resolution XPS spectra with Gaussian fitting for (b) C 1s peak, (c) N 1s peak, and (d) Ni 2p peak of Pd@N-C nanocatalyst

The presence of secondary carbons and N-containing groups present on the surface of the carbon was confirmed by the peak at 285.9 eV while the peak at 287.9 eV confirmed the bonding of the carbon atoms to N/O (C-N, C-O, C=O) which arise from the partial

decomposition of the polysaccharide chain.[22] The high-resolution spectrum of the nitrogen also showed three peaks i.e. pyridinic N (398.3 eV), pyrollic N (399.5 eV) and graphitic N, i.e. pyridinium nitrogen of condensed polycycles (400.8 eV) (Figure 4c); observed from deconvolution of the N 1s spectrum.[23] The doping of the nitrogen in the carbon framework as a result of the high-temperature carbonization of the chitosan-Ni complex gave rise to the majorly pyridinic and graphitic type of nitrogen. The deconvolution of the Ni spectrum showed three energy bands in doublets. The characteristic peak for metallic nickel can be observed at 852.1 eV. The doublet at 853.5 eV and 854 eV can be attributed to Ni^{2+} and the peaks at 855.1 and 871.3 for the Ni^{3+}.[24] The O 1s spectrum was deconvoluted to give four different peaks. The bulk CHN quantitative analysis showed the presence of 67.84% C, 1.427% H and 5.70% N in the sample.

Catalyst performance. The catalytic activity of the synthesized Ni@N-CNT was performed for the hydrogenation of nitrobenzene as a model substrate using molecular hydrogen (Scheme 2). Aniline and its derivatives are important for the synthesis of various agricultural products, drugs, dyes, polyurethanes, etc.[11]
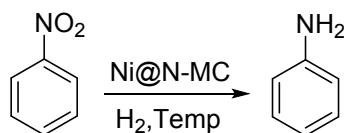
Scheme 2. Hydrogenation of nitrobenzene using molecular hydrogen.

Initially, different solvents were scrutinized for the hydrogenation of nitrobenzene. When THF was used as the solvent, no conversion of nitrobenzene was observed (Table 1, entry 1). In water, only 5% conversion of nitrobenzene was observed (Table 1, entry 2), while a mixture of water and THF (1:1) furnished only 5% conversion (Table 1, entry 3). With acetonitrile, 25% of nitrobenzene was converted to aniline with >99% selectivity (Table 1, entry 4). Notably, the hydrogenation of nitrobenzene in methanol provided better results in terms of conversion (33%) (Table 1, entry 5). This may be attributed to the higher solubility of molecular hydrogen in methanol. Thus, methanol was selected as the solvent for further studies. When the temperature of the reaction was increased from room temperature (30 °C) to 50 °C, the conversion of nitrobenzene also increased to 85% in 60 min (Table 1, entry 6). A further increase in time to 90 min, complete conversion of nitrobenzene was achieved (Table 1, entry 7). When the temperature was further increased to 80 °C, a complete conversion of nitrobenzene was observed in just 45 min (Table 1, entry 12). Also, the effect of molecular hydrogen pressure was studied by varying it in the range of 2 to 10 bar. When the pressure of the molecular hydrogen was kept at 2 bar, 65% conversion of nitrobenzene was observed in 90 min (Table 1, entry 8). The increase in the conversion of nitrobenzene can be attributed to the probability of an effective reaction with the increase of in H_2 pressure. The conversion of the nitrobenzene increased to 85% on increasing hydrogen pressure to 5 bar in 90 min (Table 1, entry 6)

while at 10 bar hydrogen pressure, the complete conversion was obtained in only 60 min (Table 1, entry 9). However, to avoid higher pressure, a 5 bar hydrogen pressure was selected as the working pressure for further catalytic studies. Next, the catalytic amount was varied to study its effect on the hydrogenation of nitrobenzene. An increment in the conversion of the nitrobenzene was observed with the increase in the catalytic amount from 12.5 mg to 25 mg (Table 1, entries 6, 10 and 11). However, on further increasing the catalyst amount, no noticeable change in the conversion or selectivity was observed (Table 1, entry 11).

Table 1 Effect of different reaction parameters on nitrobenzene hydrogenation.[a]

Entry	Temp. (°C)	Time (min)	P_{H_2} (bar)	Solvent	Cat. Amt. (mg)	Conv. (%)	Sel. (%)
1.	35	60	5	THF	25	Nd	Nd
2.	35	60	5	Water	25	5	>99
3.	35	60	5	1:1 Water:THF	25	5	>99
4.	35	60	5	Acetonitrile	25	25	>99
5.	35	60	5	Methanol	25	33	>99
6.	50	60	5	Methanol	25	85	>99
7.	50	90	5	Methanol	25	>99	>99
8.	50	90	2	Methanol	25	65	>99
9.	50	60	10	Methanol	25	>99	>99
10.	50	90	5	Methanol	12.5	65	>99
11.	50	90	5	Methanol	50	>99	>99
12.	80	45	5	Methanol	25	>99	>99
13.	50	180	5	Methanol	0	Nd	Nd

[a] **Reaction conditions:** 2 mmole nitrobenzene, 20 mL solvent, 2.4 wt.% Ni@N-CNT and 800 rpm. Nd = Not detected

Additionally, as a control experiment, the hydrogenation of nitrobenzene was carried out in the absence of the catalyst, which provided almost no conversion even after 3 h of reaction time (Table 1, entry 13). In another experiment, the catalyst was separated from the reaction mixture after 1 h of reaction time and the reaction mixture was again transferred to the reactor. The conversion at this time was 85%. The reaction mixture was further allowed to react for 1h under a hydrogen atmosphere, which gave only ~0.9% conversion, which correlates well with the background activity. These experiments, thus, prove that the reaction was indeed catalyzed by the Ni nanoparticles.

The high activity of the catalyst can be attributed to the metal-catalyzed hydrogenation reaction involving the flow of electrons between metal and the reactants.[25] The interaction of the metal with the *N*-doped carbon materials has been broadly reported in the literature. The high activity and stability of the catalyst may be attributed to the heterojunction formation between the closely associated Ni metal and the *N*-doped carbon support.[25] The fine-tuning of the properties of the metal and its support can enhance the activity of the catalyst. The Ni metal having higher Fermi energy level spontaneously donates electrons to the semiconducting *N*-doped carbon until an equilibrium is reached as shown in Scheme 3 inset. Usually the metal has a lower work function as compared to the *N*-doped carbon, thus having a restricted flow of electrons as

compared to the metallic conductor.[26] This phenomenon is termed as Mott-Schottky effect. The close contact formed at the heterojunction of nickel and *N*-doped carbon bring about an electron redistribution, thus increasing the positive charge on the metal making it electron deficient in nature. This establishes a charge region at the interface of the nickel-metal and carbon, which was responsible for the selective hydrogenation.
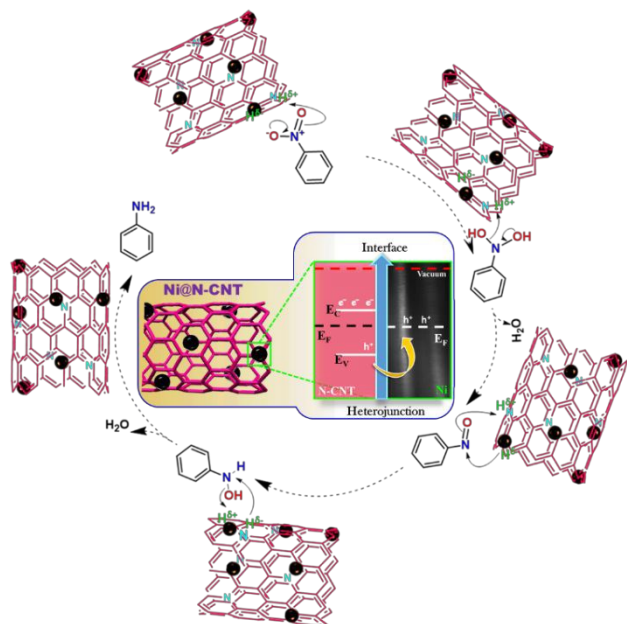
Scheme 3. Plausible mechanistic steps in the hydrogenation of nitrobenzene and the center, the formation of Mott-Schottky junction between the surface Ni metal and N-doped CNT.
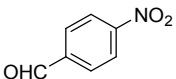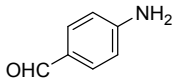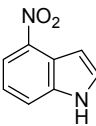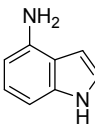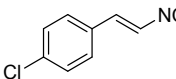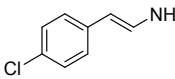
Looking at the escalation in the amount of various anthropogenic nitroarene pollutants from the industry, researchers have focussed on the reduction of these compounds to corresponding amines that find applications in the synthesis of various drugs, photographic development, anti-corrosive additives in paints, and many more.[27] With this in mind, we evaluated the catalytic reduction of various nitroarene substrates giving the corresponding products as confirmed by GC and GC-MS (Figure S1-12 in the ESI) under the optimized reaction conditions using the synthesized catalyst. It was observed that hydrogenation of the nitrobenzene occurred even at 50 °C while hydrogenation of the solid substrates required a higher reaction temperature (80 °C) for their activation. This may be attributed to the higher solubility of the molecular hydrogen directly in the nitrobenzene as that compared to the other substrates. Thus, hydrogenation was carried at 80 °C for the rest of the molecules. For comparison purposes, the hydrogenation of nitrobenzene was carried out under the optimized conditions using 2.5 mg of catalyst (similar mole % to that present in the Ni@N-CNT). No conversion of nitrobenzene was observed even after 1 h. However, upon increasing the amount of Raney-Ni to 10 mg, 20% conversion of nitrobenzene was observed at 80 °C. The hydrogenation of 4-nitrotoluene and 4-ethyl nitrobenzene contributed nearly complete conversion along with complete

selectivity towards the corresponding aniline (Table 2, entries 3 and 4). The catalytic hydrogenation of a 4-nitrophenol, one of the priority pollutant, was also tested.[28] This toxic and carcinogenic substrate was completely reduced to the corresponding amine in 2.5 h. The hydrogenating ability of the Ni@N-CNT nanocatalyst was also checked with chlorine substituted nitrobenzene (Table 2, entry 6). The catalyst converted 4-chloro nitrobenzene into 4-chloroaniline selectively with no dechlorinated product, which is a common issue in the hydrogenation of such chlorinated substrates. The selective synthesis of 4-chloroaniline is of utter importance in the industry as it is one of the important intermediates for the synthesis of an antimalarial drug like paludrine.[29] The chemoselectivity in this case may be attributed to the N-doping in the CNT's. The nitrogen doping in the CNT generates an increase in the electron density at the neighbouring stabilized Ni metal making it electron-rich. The dechlorination generally occurs via dissociative adsorption of C-Cl bond. The electrostatic repulsion between C-Cl moiety and electron-enriched Ni sites and/or destabilization of the transition state inhibit dechlorination.

Table 2 The scope of the hydrogenation of various substrates catalyzed by Ni@N-CNT nanocatalyst.[a]

Ent.	Substrate	Product	Time (h)	% Sel.	IY[d] (%)
1.	NO₂	NH₂	0.75	>99	93
2.	NO₂	NH₂	[b] 1	Nd	-
			[c] 1	>99	-
3.	NO₂ (4-methyl)	NH₂ (4-methyl)	2	>99	90
4.	NO₂ (4-ethyl)	NH₂ (4-ethyl)	1	>99	92
5.	HO–NO₂	HO–NH₂	2.5	>99	96
6.	Cl–NO₂	Cl–NH₂	1.5	>99	92
7.	O₂N–NO₂	H₂N–NH₂	2	>99	95
8.	H₂N–NO₂	H₂N–NH₂	1.5	>99	94
9.	H₂NO₂S–NO₂	H₂NO₂S–NH₂	15.5	>99	80
10.	NO₂ (naphthalene)	NH₂ (naphthalene)	3.5	>99	95
11.	NC–NO₂	NC–NH₂	2.5	>99	90

12.	(4-NO$_2$, OHC-phenyl)	(4-NH$_2$, OHC-phenyl)	5	>99	85
13.	(4-nitro indole)	(4-amino indole)	14.5	>99	83
14.	(4-Cl, NO$_2$-styryl)	(4-Cl, NH$_2$-styryl)	15.5	>99	79

[a] **Reaction conditions:** 2 mmole nitrobenzene, 20 mL methanol, 2.4 wt.% Ni@N-CNT 800 rpm, >99% conversion. [b] 2.5 mg Raney Ni, No conversion. [c] 10 mg Raney Ni, 20% conversion. [d]IY=Isolated yield

Next, the hydrogenation of 4-amino nitrobenzene and 1,4-dinitrobenzene carried out using the Ni@N-CNT catalyst gave almost complete conversion of the substrates to 1,4-phenylenediamine (Table 2, entries 7 and 8). The reduction of 4-nitrobenzensulfonamide and 1-nitronaphthalene also displayed high conversion and selectivity using the Ni@N-CNT catalyst (Table 2, entries 9 and 10). To, check the chemoselectivity of the products we hydrogenated various nitroarenes which were already substituted by other reducible functionalities like –CHO, –CN, etc. The hydrogenation of 4-nitrobenzonitrile selectively furnished 4-cyanoaniline (Table 2, entry 11). Similarly, the Ni@N-CNT catalyzed hydrogenation of 4-nitrobenzaldehyde offered selectively 4-aminobenzaldehyde (Table 2, entry 12). No reduction of –CHO or –CN group occurred using the as-synthesized catalyst. In addition, the reduction of nitro group in the heterocyclic system (Table 2, entry 13) was achieved with high conversion and selectivity towards corresponding amine.

The plausible reaction mechanism for the hydrogenation of nitrobenzene is shown in Scheme 3. The hydrogenation of nitrobenzene involves four successive steps to give aniline. The first step involves a polar reaction mechanism wherein molecular hydrogen undergoes heterolytic cleavage via synergic activity between Ni nanoparticles and the N-doped CNT, resulting in high activity of the catalyst towards selective formation of amine products.

Recently Lan et al. used hollow yolk-shell Co-N-C@SiO$_2$ Nanoreactors synthesized from ZIF-67 as template and SiO$_2$ support with varying Co metal (10-25%) content for the selective hydrogenation of nitroarenes.[30] The catalyst was ~3.3 times active as compared to the Co/SiO$_2$. In a similar manner, Sun et al. used single cobalt sites on mesoporous N-doped carbon matrix for selective catalytic hydrogenation of nitroarenes which again used Zn/Co bimetallic ZIF MOF and SiO$_2$ support.[31] The ICP analysis of the reaction mixture showed around 3 % leaching of the active Co metal after each run. However, both of these catalysts contained large metal loading % along with the use of expensive MOF for the synthesis of N-doped carbon at higher reaction temperature (110 °C) and pressure (30 MPa). The higher activities of both of these catalysts were attributed to the Co-N$_x$ species present in the catalyst. In a recent study, Ni nanoparticles were stabilized on the carboxylic acid modified siliceous (2D hexagonal mesoporous SBA-15C and 3D cage-type SBA-16C) supports and used for the

hydrogenation of nitroarenes using NaBH$_4$ as the hydrogen source.[32] Ni NPs supported within the 3D cage-type mesopores of SBA-16C showed higher catalytic activities as compared to the 2D analogue in the reduction of nitroarenes. However, the catalyst activity was not precisely generalized in terms of structure of the channels/pores of the catalyst. Also, the waste production associated with the usage of NaBH$_4$ as hydrogen source cannot be ruled out. An atomically dispersed Ni (~4.5%) on the N-doped porous carbon was used for the selective hydrogenation of nitroarenes.[30] Yet again, the reduction temperature was as high as 120 °C with molecular hydrogen pressure of 3 MPa. Also, the catalyst synthesis was done by a hard template method followed by the sulphuric and nitric acid treatment to obtain the final catalyst. Thus, compared to these catalysts, the Ni@N-CNT catalyst in this report shows similar catalytic activity at low reaction temperature (80 °C) as well as molecular hydrogen pressure (0.5 MPa) towards the chemoselective reduction of various nitroarenes to corresponding aminoarenes.

We followed the similar synthetic method to synthesize Nickel nanoparticles on N-doped carbon nanotubes via pyrolysis of Ni impregnated chitosan for the hydrogenation of various nitroarenes at lower reaction temperature and H$_2$ pressure as compared to the conventional protocols using higher temperature and H$_2$ pressure. To the best of our knowledge, there exist only one report where the biomass waste was directly used for the gram scale synthesis of CNT at a lower temperature and utilized for the oxidation reduction reaction catalyst [34].

The recovery and recyclability of the catalyst is not only important from the economic point of view but also from the ecological perspective. The recyclability of the Ni@N-CNT nanocatalyst was verified for the hydrogenation of nitrobenzene as a model reaction (Figure S12 in the ESI). For the reusability experiments, the catalyst was separated using an external magnetic field, washed with methanol and vacuum dried at 50 °C. No significant change in the selectivity of aniline was observed using the regenerated catalyst. The ICP-OES analysis of the reaction mixture showed the absence of nickel in the reaction mixture.

Conclusions

To conclude, we have developed a simple methodology for the in-situ formation of nickel nanoparticles capped on the N-doped carbon obtained via scale-up strategy using single step pyrolysis of chitosan as a single source of carbon and nitrogen. The doping of nitrogen in the carbon nanotube network provides an adsorption site for the formation of closely coupled, highly stable and uniform nickel nanoparticles. A strong electronic interaction of the Ni^0 and N-doped carbon nanotubes. The non-noble nickel nanoparticles in the N-doped carbon offer abundant reactive sites for nitroarene adsorption along with diffusion and dissociation of molecular hydrogen. The catalyst successfully and chemoselectively hydrogenated the nitroarenes to corresponding amines at moderate pressure (5 bar) and comparatively low temperature. The catalyst was

highly recyclable and did not show any leaching of the Ni metal even after five cycles.

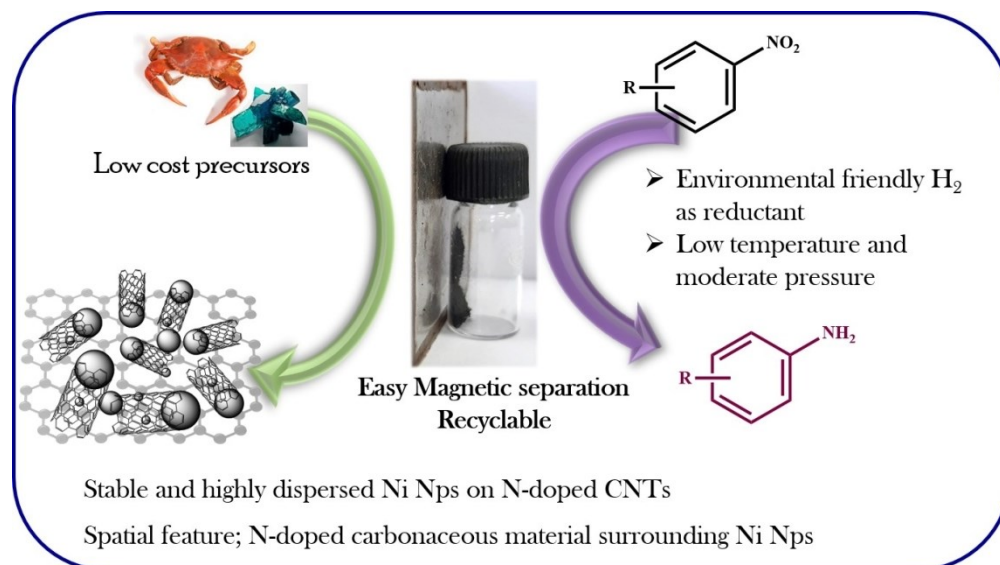## Conflicts of interest

There are no conflicts to declare.

Acknowledgements

References

[1] a) E. Guibal, Heterogeneous catalysis on chitosan-based materials: a review. *Prog. Polym. Sci.* 2005, **30**, 71; b) R. Jayakumar, D. Menon, K. Manzoor, S. V. Nair, H. Tamura, Biomedical applications of chitin and chitosan based nanomaterials-A short review. *Carbohydr. Polym.* 2010, **82**, 227; c) A. El Kadib, Chitosan as a Sustainable Organocatalyst: A Concise Overview. *ChemSusChem* 2015, 8, 217.

[2] a) L. Wang, B. Zhang, X. Meng, D. S. Su, F. S. Xiao, Hydrogenation of biofuels with formic acid over a palladium-based ternary catalyst with two types of active sites. *ChemSusChem* 2014, **7**, 1537; b) Y. Wang, Q. Liu, M. Xu, G. Shu, M. Jiang, G. Fei, M. Zeng, Carbonization of Chitosan in Palladium-Chitosan/ Montmorillonite Composites to Prepare Novel Heterogeneous Catalysts for Heck Reactions. *J. Macromol. Sci. Part B Phys.* 2017, **56**, 670; c) B. Sahoo, A. E. Surkus, M. M. Pohl, J. Radnik, M. Schneider, S. Bachmann, M. Scalone, K. Junge, M. Beller, A Biomass-Derived Non-Noble Cobalt Catalyst for Selective Hydrodehalogenation of Alkyl and (Hetero)Aryl Halides. *Angew. Chem. Int. Ed.* 2017, **56**, 11242; d) J. H. Advani, N. H. Khan, H. C. Bajaj, A. V. Biradar, Stabilization of palladium nanoparticles on chitosan derived N-doped carbon for hydrogenation of various functional groups. *Appl. Surf. Sci.* 2019, **487**, 1307. e) J. H. Advani, A. S. Singh, N. H. Noor-ul, H. C. Bajaj, A. V. Biradar, Black yet green: Sulfonic acid functionalized carbon as an efficient catalyst for highly selective isomerization of α-pinene oxide to trans-carveol. *Appl. Catal. B*, 2020, **268**, 118456.

[3] S. Abdalla, F. Al-Marzouki, A. A. Al-Ghamdi, A. Abdel-Daiem, Different Technical Applications of Carbon Nanotubes. *Nanoscale Res. Lett.* 2015, **10**, 358.

[4] T. Guo, P. Nikolaev, A. Thess, D. T. Colbert, R. E. Smalley, Catalytic growth of single-walled manotubes by laser vaporization. *Chem. Phys. Lett.* 1995, **243**, 49.

[5] S. Y. Lim, M. M. Norani, The Effect of Catalyst on Carbon Nanotubes (CNTs) Synthesized by Catalytic Chemical Vapor Deposition (CVD) Technique. *Adv. Mater. Res.* 2011, **364**, 232.

[6] T. X. Li, K. Kuwana, K. Saito, H. Zhang, Z. Chen, Temperature and carbon source effects on methane-air flame synthesis of CNTs. *Proc. Combust. Inst.* 2009, **32**, 1855.

[7] S. Iijima, Helical microtubules of graphitic carbon. *Nature* 1991, **354**, 56.

[8] a) R. Arrigo, M. E. Schuster, Z. L. Xie, Y. M. Yi, G. Wowsnick, L. L. Sun, K. E. Hermann, M. Friedrich, P. Kast, M. Havecker, A. Knop-Gericke, R. Schlogl, Nature of the N–Pd Interaction in Nitrogen-Doped Carbon Nanotube Catalysts. *ACS Catal.* 2015, **5**, 2740; b) M. Sankaran, B. Viswanathan, The role of heteroatoms in carbon nanotubes for hydrogen storage. *Carbon* 2006, **44**, 2816.

[9] a) Y. Gao, G. Hu, J. Zhong, Z. Shi, Y. Zhu, D. S. Su, J. Wang, X. Bao, D. Ma, Nitrogen-Doped sp^2-Hybridized Carbon as a Superior Catalyst for Selective Oxidation. *Angew. Chem. Int. Ed.* 2013, **52**, 2109; b) S. Yang, L. Peng, P. Huang, X. Wang, Y. Sun, C. Cao, W. Song, Nitrogen, phosphorus, and sulfur co-doped hollow carbon shell as superior metal-free catalyst for selective oxidation of aromatic alkanes. *Angew. Chem. Int. Ed.* 2016, **55**, 4016; c) J. P. Paraknowitsch, A. Thomas, M. Antonietti, A detailed view on the polycondensation of ionic liquid monomers towards nitrogen doped carbon materials. *J. Mater. Chem.* 2010, 20, 6746.

[10] A. M. Doyle, S. K. Shaikhutdinov, S. D. Jackson, H. J. Freund, Hydrogenation on Metal Surfaces: Why are Nanoparticles More Active than Single Crystals? *Angew. Chem. Int. Ed.* 2003, **42**, 5240.

[11] a) B. Amini, S. Lowenkron, *Kirk-Othmer Encyclopedia of Chemical Technology* 2000; b) A. Corma, P. Serna, Chemoselective hydrogenation of nitro compounds with supported gold catalysts. *Science*, 2006, **313**, 332.

[12] a) M. Orlandi, D. Brenna, R. Harms, S. Jost, M. Benaglia, Recent Developments in the Reduction of Aromatic and Aliphatic Nitro Compounds to Amines. *Org. Process Res. Dev.* 2016, **22**, 430; b) B. Priewisch, K. Ruck-Braun, Efficient Preparation of Nitrosoarenes for the Synthesis of Azobenzenes. *J. Org. Chem.* 2005, **70**, 2350. c) D. Formenti, F. Ferretti, F. K. Scharnagl, M. Beller, Reduction of Nitro Compounds Using 3d-Non-Noble Metal Catalysts. *Chem. Rev.* 2019, **119**, 2611; d) R. V. Jagadeesh, K. Murugesan, A. S. Alshammari, H. Neumann, M. M. Pohl, J. Radnik, M. Beller. MOF-derived cobalt nanoparticles catalyze a general synthesis of amines. *Science* 2017, **358**, 326; e) R.V. Jagadeesh, A. E., Surkus, H. Junge, M. M. Pohl, J. Radnik, J. Rabeah, H. Huan, V. Schünemann, A. Brückner, M. Beller, Nanoscale Fe_2O_3-based catalysts for selective hydrogenation of nitroarenes to anilines. *Science*, 2013, **342**, 1073; f) F. A. Westerhaus, R. V. Jagadeesh, G. Wienhofer, M. M. Pohl, J. Radnik, A. E. Surkus, J. Rabeah, K. Junge, H. Junge, M. Nielsen, A. Brukner, Heterogenized Cobalt oxide catalysts for the nitroarene reduction by pyrolysis of molecularly defined complexes. *Nat. Chem.*, 2013, **5**, 537.

[13] a) V. M. Roberts, V. Stein, T. Reiner, A. Lemonidou, X. Li, J. A. Lercher, Towards quantitative catalytic lignin depolymerization. *Chemistry* 2011, **17**, 5939; b) C. Zhao, J. A. Lercher, Upgrading pyrolysis oil over Ni/HZSM-5 by cascade reactions. *Angew. Chem. Int. Ed.* 2012, **51**, 5935.

[14] a) H. Fei, Y. Yang, Z. Peng, G. Ruan, Q. Zhong, L. Li, E. L. Samuel, J. M. Tour, Cobalt Nanoparticles Embedded in

Nitrogen-Doped Carbon for the Hydrogen Evolution Reaction. *ACS Appl. Mater. Interfaces* 2015, **7**, 8083; b) K. K. Datta, B. V. Reddy, K. Ariga, A. Vinu, Gold nanoparticles embedded in a mesoporous carbon nitride stabilizer for highly efficient three-component coupling reaction. *Angew. Chem. Int. Ed.* 2010, **49**, 5961; c) L. R. Baker, G. Kennedy, M. Van Spronsen, A. Hervier, X. Cai, S. Chen, L. W. Wang, G. A. Somorjai, Furfuraldehyde Hydrogenation on Titanium Oxide-Supported Platinum Nanoparticles Studied by Sum Frequency Generation Vibrational Spectroscopy: Acid–Base Catalysis Explains the Molecular Origin of Strong Metal–Support Interactions. *J. Am. Chem. Soc.* 2012, **134**, 14208.

[15] B. Hoffer, The role of the active phase of Raney-type Ni catalysts in the selective hydrogenation of d-glucose to d-sorbitol. *Appl. Catal., A* 2003, **253**, 437.

[16] a) A. El Kadib, K. Molvinger, M. Bousmina, D. Brunel, Decoration of chitosan microspheres with inorganic oxide clusters: Rational design of hierarchically porous, stable and cooperative acid–base nanoreactors. *J. Catal.* 2010, **273**, 147; b) E. Guibal, Interactions of Metal Ions with Chitosan-Based Sorbents: A Review. *Sep. Purif. Technol.* 2004, **38**, 43.

[17] J. Lahiri, T. S Miller, A. J Ross, L. Adamska, I. I. Oleynik, M. Batzill, Graphene growth and stability at nickel surfaces. *New J. Phys.* 2011, 13.

[18] a) K. Jasuja, V. Berry, Implantation and Growth of Dendritic Gold Nanostructures on Graphene Derivatives: Electrical Property Tailoring and Raman Enhancement. *ACS Nano* 2009, **3**, 2358; b) A. C. Ferrari, J. C. Meyer, V. Scardaci, C. Casiraghi, M. Lazzeri, F. Mauri, S. Piscanec, D. Jiang, K. S. Novoselov, S. Roth, A. K. Geim, Raman Spectrum of Graphene and Graphene Layers. *Phys. Rev. Lett.* 2006, **97**, 187401.

[19] a) J. Robertson, Amorphous carbon. *Adv. Phys.* 1986, 35, 317; b) W. M. Silva, H. Ribeiro, L. M. Seara, H. D. R. Calado, A. S. Ferlauto, R. M. Paniago, C. F. Leite, G. G. Silva, Surface Properties of Oxidized and Aminated Multi-Walled Carbon Nanotubes. *J. Braz. Chem. Soc.* 2012, **23**, 1078; c) F. Tuinstra, J. L. Koenig, Raman Spectrum of Graphite. *J. Chem. Phys.* 1970, **53**, 1126.

[20] a) L. Bokobza, J. Zhang, Raman spectroscopic characterization of multiwall carbon nanotubes and of composites. *Express Poly. Lett.* 2012, **6**, 601; b) M. S. Mohamed Saheed, N. M. Mohamed, Z. A. Burhanudin, Effect of Different Catalyst Deposition Technique on Aligned Multiwalled Carbon Nanotubes Grown by Thermal Chemical Vapor Deposition. *J. Nanomater.* 2014, 707301.

[21] M. Wang, H. Li, Y. Wu, J. Zhang, Comparative studies on the catalytic behaviors between the Ni–B amorphous alloy and other Ni-based catalysts during liquid phase hydrogenation of acetonitrile to ethylamine. *Mater. Lett.* 2003, **57**, 2954.

[22] S. Y. Gao, H. Fan, X. J. Wei, L. Li, Y. Bando, D. Golberg, Nitrogen-Doped Carbon with Mesopore Confinement Efficiently Enhances the Tolerance, Sensitivity, and Stability of a Pt Catalyst for the Oxygen Reduction Reaction *Part. Part. Syst. Char.* 2013, **30**, 864.

[23] a) A. Primo, P. Atienzar, E. Sanchez, J. M. Delgado, H. Garcia, From biomass wastes to large-area, high-quality, N-doped graphene: catalyst-free carbonization of chitosan coatings on arbitrary substrates. *Chem. Commun.* 2012, 48,

9254; b) B. Xiong, Y. K. Zhou, Y. Y. Zhao, J. Wang, X. Chen, R. O'Hayre, Z. P. Shao, The use of nitrogen-doped graphene supporting Pt nanoparticles as a catalyst for methanol electrocatalytic oxidation. *Carbon* 2013, **52**, 181.

[24] a) L. Yu, Q. Yi, X. Yang, Y. Chen, An easy synthesis of Ni-Co doped hollow C-N tubular nanocomposites as excellent cathodic catalysts of alkaline and neutral zinc-air batteries. *Sci. China Mater.* 2019, 62, 1251; b) X.-F. Lu, D.-J. Wu, R.-Z. Li, Q. Li, S.-H. Ye, Y.-X. Tong, G.-R. Li, Hierarchical NiCo 2 O 4 nanosheets@ hollow microrod arrays for high-performance asymmetric supercapacitors. *J. Mater. Chem. A* 2014, **2**, 4706.

[25] X. H. Li, M. Antonietti, Metal nanoparticles at mesoporous N-doped carbons and carbon nitrides: functional Mott–Schottky heterojunctions for catalysis. *Chem. Soc. Rev.* 2013, **42**, 6593.

[26] a) D. Deng, L. Yu, X. Chen, G. Wang, L. Jin, X. Pan, J. Deng, G. Sun, X. Bao, Iron encapsulated within pod-like carbon nanotubes for oxygen reduction reaction. *Angew. Chem. Int. Ed.* 2013, 52, 371; b) T. Chen, S. Guo, J. Yang, Y. Xu, J. Sun, D. Wei, Z. Chen, B. Zhao, W. Ding, Nitrogen-Doped Carbon Activated in Situ by Embedded Nickel through the Mott-Schottky Effect for the Oxygen Reduction Reaction. *Chemphyschem* 2017, **18**, 3454.

[27] H. Hu, J. H. Xin, H. Hu, X. Wang, D. Miao, Y. Liu, Synthesis and stabilization of metal nanocatalysts for reduction reactions – a review. *J. Mater. Chem. A* 2015, **3**, 11157.

[28] a) T. Aditya, A. Pal, T. Pal, Nitroarene reduction: a trusted model reaction to test nanoparticle catalysts. *Chem. Commun.* 2015, **51**, 9410; b) X. Le, Z. Dong, Y. Liu, Z. Jin, T.-D. Huy, M. Le, J. Ma, Palladium nanoparticles immobilized on core–shell magnetic fibers as a highly efficient and recyclable heterogeneous catalyst for the reduction of 4-nitrophenol and Suzuki coupling reactions *J. Mater. Chem. A* 2014, **2**, 19696.

[29] J. K. Baird, S. L. Hoffman, Primaquine therapy for malaria. *Clin. Infect. Dis.* 2004, **39**, 1336.

[30] X. Lan, B. Ali, Y. Wang, T. Wang, Hollow and Yolk−Shell Co-N-C@SiO₂ Nanoreactors: Controllable Synthesis with High Selectivity and Activity for Nitroarene Hydrogenation. *ACS Appl. Mater. Interfaces.* 2020, **12**, 3624−3630.

[31] X. Sun, A. I. Olivos-Suarez, D. Osadchii, M. J. V. Romero, F. Kapteijn, J. Gascon, Single cobalt sites in mesoporous N-doped carbon matrix for selective catalytic hydrogenation of nitroarenes. *J. Catal.*, 2018, **357**, 20-28.

[32] C. S. Budi, D. Saikia, C. S. Chen, H. M. Kao, Catalytic evaluation of tunable Ni nanoparticles embedded in organic functionalized 2D and 3D ordered mesoporous silicas from the hydrogenation of nitroarenes. *J. Catal*. 2019, **370**, 274-288.

[33] F. Yang, M. Wang, W. Liu, B. Yang, Y. Wang, J. Luo, Y. Tang, L. Hou, Y. Li, Z. Li, B. Zhang, W. Yang, Y. Li, Atomically dispersed Ni as the active site towards selective hydrogenation of nitroarenes. *Green Chem*. 2019, **21**, 704-711.

[34] Y. Zhang, L. Lu, S. Zhang, Z. Lv, D. Yang, J. Liu, Y. Chen, X. Tian, H. Jin, W. Song, Biomass chitosan derived cobalt/nitrogen doped carbon nanotubes for the electrocatalytic oxygen reduction reaction. *J. Mater. Chem. A*, 2018, 6, 5740.

234x131mm (150 x 150 DPI)